Analysis, numerics, and optimization of algae growth

Document Version:
Publisher's PDF, also known as Version of Record (includes final page, issue and volume numbers)

Please check the document version of this publication:

• A submitted manuscript is the version of the article upon submission and before peer-review. There can be important differences between the submitted version and the official published version of record. People interested in the research are advised to contact the author for the final version of the publication, or visit the DOI to the publisher's website.
• The final author version and the galley proof are versions of the publication after peer review.
• The final published version features the final layout of the paper including the volume, issue and page numbers.

[Link to publication](#)

EINDHOVEN UNIVERSITY OF TECHNOLOGY
Department of Mathematics and Computer Science

CASA-Report 10-74
December 2010

Analysis, numerics, and optimization of algae growth

by

K. Kumar, M. Pisarenco, M. Rudnaya, V. Savcenco

Analysis, numerics, and optimization of algae growth

Kundan Kumar, Maxim Pisarenco, Maria Rudnaya, Valeriu Savcenco

Technische Universiteit Eindhoven, P.O. Box 513, 5600 MB Eindhoven, The Netherlands

Abstract

We extend the mathematical model for algae growth as described in [11] to include new effects. The roles of light, nutrients and acidity of the water body are taken into account. Important properties of the model such as existence and uniqueness of solution, as well as boundedness and positivity are investigated. We also discuss the numerical integration of the resulting system of ordinary differential equations and derive a condition which guarantees positivity of the numerical solution. An optimization problem is formulated which demonstrates an application of the model.

1 Introduction

Existing models for algae growth can be categorized into two groups. The first group, of "soft models", consists of models derived from first principles and heuristic assumptions without relying on validation with experimental data. The models in the second group are referred to as "hard models" and are designed by fitting the parameters of the model to real data. A prominent representative of the first group is the model proposed by Huisman and Weissing [7]. It was one of the first to recognize the role of depth-dependence of light intensity on the dynamics of algae population. In this work, the algae concentration is averaged across the vertical direction. This made the model simple but also less realistic. A later paper [12] extended this work to a full three-dimensional model which could account for mixing in all directions.

Malve et al [10] and Haario et al [3] applied the "hard modeling" approach to the analysis of an algae growth problem. The algae dynamics was modeled as a nonlinear system of ordinary differential equations (ODEs) with parameters fitted to data consisting of eight years of observations. The model incorporates reaction rate dependence on the temperature, but neglects the effects of light attenuation with depth.

In our model we consider the algae concentration to be depth-dependent, leading to a partial differential equation in space and time. The main factors which influence the amount of algae biomass B are the concentrations of phosphates P, nitrates N, and carbon dioxide C in the water as well as the intensity of light.

$$N + P + C \xrightarrow{light} B.$$

1

The light intensity has no direct effect on the the nutrients (N and P) and the carbon dioxide, which are also assumed to have a large diffusion rate. This implies that their concentration may be considered space-independent and the ODEs with coefficients fitted to experimental data from [3] may be incorporated into our model. This allows realistic reaction rates and reliable output.

The proposed model offers insight on the influence of mixing and of the pH on the growth rate. The pH of the medium can be controlled by adding carbon dioxide, which may be taken as an input parameter in an optimization problem.

The paper is organized as follows. In Section 2 the mathematical model is presented. Section 3 is concerned with the analysis of the model. A numerical scheme is proposed in Section 4 together with conditions which guarantee positivity of the numerical solution. Sections 5 and 6 demonstrate respectively numerical experiments and the optimization of growth with respect to the amount of minerals and carbon dioxide. Finally our conclusions are presented in the Section 7.

2 Mathematical model

We model the growth of the algae (biomass) in the water body. The biomass growth rate is related to the process of photosynthesis, the process of mixing, and the death rate. The process of photosynthesis depends on the concentration of the nutrients, the availability of carbon dioxide and the availability of light. The death rate includes both the harvesting rate as well as the natural death rate of the algae. Since the light intensity is uneven at different depths of the water, it is important to stir the water causing the mixing of the algae. In our model advection is assumed to be absent.

In the horizontal plane, we consider no variation and hence, the growth rate is independent of x and y coordinates. Thus, it is sufficient to consider a one-dimensional domain denoted by $\Omega = [0, z_{max}]$, where z_{max} is the depth of the water body.

In our model the growth rate w of the algae biomass is given by

$$\partial_t w = g(I_{\text{in}})f_1(P)f_2(N)f_3(C)w + D_M\partial_{zz}w - H_a(w, C), \tag{1}$$

where I_{in}, P, N and C are respectively the light intensity, the concentrations of phosphorus, nitrogen and carbon dioxide. The mixing is modeled by a diffusion term with a constant coefficient D_M. Inclusion of the mixing term helps to understand the effect of mixing on the overall production rate of the algae. The functions $g(I_{\text{in}})$, $f_1(P)$, $f_2(N)$ and $f_3(C)$ define the dependence of the biomass growth rate on the light intensity, the concentration of nutrients (phosphates and nitrates) and the carbon dioxide. The function H_a models the depletion rate of algae biomass and includes both the harvesting and the natural decay. A similar model is used in [6, 11]. Following [5] the effect of light intensity on the biomass growth is modelled by a Monod function (see [14], [12]),

$$g(I_{\text{in}}) = \frac{\mu_0 I_{\text{in}}}{H_L + I_{\text{in}}}, \tag{2}$$

2

where I_{in} is the effective light intensity received by the algae and H_L is the half-saturation intensity. The Monod form ensures that the growth rate is almost linear when the light intensity is very small, and that the growth rate remains bounded by μ_0 when I_{in} becomes very large. Figure 1 illustrates a family of Monod functions for different half-saturation constants. The light intensity received by the algae is not uniform throughout the water body. The light intensity is attenuated by two factors: the presence of algae and the water surface. The presence of the algae in the top layers causes reduction in the available light for the algae in the deeper layers. Moreover, the water layers themselves cause attenuation in the available light intensity for the deeper layers. Considering the above discussions, the light intensity can be modeled by

$$I_{\text{in}}(w, z, t) = I_0(t)e^{-kz}e^{(-r_s \int_0^z w(s,t)\,ds)}, \tag{3}$$

where $I_0(t)$ is the incident light intensity which changes in time (for instance, day and night cycle). The constant k is the specific light attenuation coefficient due to the water layer and r_s is the specific light attenuation coefficient due to the presence of algae.

For the nutrients (N and P), we once again take Monod-type rates

$$f_1(P) = \frac{k_P[P - P_c]_+}{H_P + [P - P_c]_+}, \tag{4}$$

$$f_2(N) = \frac{k_N[N - N_c]_+}{H_N + [N - N_c]_+}. \tag{5}$$

Here, H_P and H_N are the half-saturation concentrations of phosphates and nitrates respectively. The $[\cdot]_+$ denotes the positive cut function $[x]_+ = \max(0, x)$. Parameters P_c and N_c are the critical concentration of the nitrates and phosphates, respectively, below which the growth becomes zero. We assume that the acidity of the water (pH value) is solely determined by the concentration of carbon dioxide. Thus, apart from the other factors discussed above, the growth rate of the algae is influenced by the pH. The consumption of carbon dioxide leads to an increase in the pH value. It is known that there is a certain range of acidity for which the algae growth is optimal. The pH may be controlled by adding carbon dioxide to the system. Hence, if more carbon dioxide than required is added, the pH value of the water will decrease. This decrease can lead to the enhancement of the decay rate of the biomass. The growth rate dependence is modeled by a function that monotonically decreases with pH (and hence monotonically increases with the concentration of carbon dioxide). However at higher concentrations of carbon dioxide the growth rate becomes constant and bounded. We consider the following function

$$f_3(C) = \frac{1}{1 + e^{(\lambda(pH(C) - pH_{dopt}))}}, \tag{6}$$

where λ is a parameter that describes the sharpness of the profile and pH_{dopt} describes the "switching" value of pH at which the growth increases if all other factors are kept
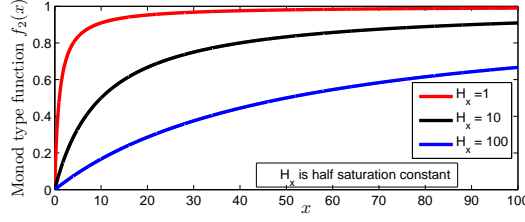
3

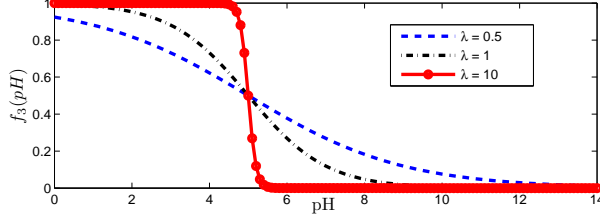Figure 1: Monod-type function for different half-saturation constants.

Figure 2: Plot of f_3 as function of pH, for different values of parameter λ.

unchanged. The relation between the pH and the concentration of carbon dioxide is given as

$$pH(C) = (6.35 - \log_{10} C)/2.$$

This relation is obtained using the chemical equilibrium constant of the hydrolysis of the carboxylic acid. The modeling of the harvesting term includes the specific death rate having pH dependence so that at small pH the death rate enhances. We propose the following functional dependence for this term similar to the $f_3(pH)$

$$H_a(w, C) = \mu_e f_4(C) w, \tag{7}$$

with μ_e being a constant and

$$f_4(C) = \frac{1}{1 + e^{(\lambda(pH(C) - pH_{dopt}))}}, \tag{8}$$

where pH_{dopt} is again the "switching" value of the pH at which the death rate increases. In Figure 2 we illustrate the nature of the f_3 function.

We complete the system with the following ordinary differential equations describing the evolution of the nutrients and the carbon dioxide

$$\frac{dN}{dt} = -\frac{1}{z_{\max}} \left(\int_0^{z_{\max}} g(I_{\text{in}}) f_1(P) f_2(N) f_3(C) w \, dz \right) N + S_N =: L_N(N, P, C, w),$$

$$\frac{dP}{dt} = -\frac{1}{z_{\max}} \left(\int_0^{z_{\max}} g(I_{\text{in}}) f_1(P) f_2(N) f_3(C) w \, dz \right) P + S_P =: L_P(N, P, C, w), \tag{9}$$

$$\frac{dC}{dt} = -\frac{1}{z_{\max}} \left(\int_0^{z_{\max}} g(I_{\text{in}}) f_1(P) f_2(N) f_3(C) w \, dz \right) C + S_C =: L_C(N, P, C, w),$$

4

where $z_{\max}$ is the maximum depth of the water body and S_N, S_P, S_C are the source terms for the nitrogen, phosphorus and carbon dioxide and for analysis purpose we set them to 0. Including these would not alter the conclusions as long as they are bounded and regular enough. These source terms are used to account for adding fertilizers or providing carbon dioxide to the pond.

We use homogeneous Neumann boundary conditions at $z = 0$ and homogeneous Dirichlet boundary conditions for $z = z_{max}$ for (1) and we require the following initial conditions

$$N(0) = N_0, \quad P(0) = P_0, \quad C(0) = C_0, \quad w(z, 0) = w_0(z). \tag{10}$$

Equations (1), (9) together with initial conditions (10) constitute the system of equations under study. We use the following values of the parameters for the numerical computations taken from [2, 5, 3].

$\mu_0 k_p k_N [1/s]$	$H_L [W/(m^2 \cdot day)]$	$H_N [g/l]$	$H_P [g/l]$
0.0886	70	$14.5 \cdot 10^{-6}$	$10.4 \cdot 10^{-6}$

$r_s [l \cdot m/g]$	$k [1/m]$	$D_M [m^2/s]$	$\mu_e [g/(l \cdot day)]$
10	0.2	$5 \cdot 10^{-4}$	0

The chosen values of the parameters are realistic [3], however, not all the parameters are exactly known and approximate values are taken for those parameters. The model is generic and for a given type of algae these parameters need to be determined experimentally. Here, we need the parameters to see whether the obtained results are realistic.

3   Analysis of the model

In this section we prove the existence and uniqueness of the solution for above model and furthermore show that the solution preserve positivity and boundedness. We first formulate the equations in the weak form and use fixed point iteration to obtain existence. The existence proof also provides bounds on the solution and its non-negative properties. Furthermore, the uniqueness proof is provided to ensure that the solution is unique. The nonstandard aspect of this model is that the model is non-local and this introduces additional complications for the proof of uniqueness.

3.1   Definition of weak solution

Further we formulate a weak form for (1)-(10). We define a function space $\mathcal{V}$

$$\mathcal{V} = L^2(0, T; H^1(\Omega))$$

and we seek for the solution $w \in \mathcal{V}$, such that $\partial_t w \in L^2(0, T; H^{-1}(\Omega))$ with $N, P, C \in H^1(0, T)$ and

$$(\partial_t w, v) + (D_M \partial_z w, \partial_z v) = (g(I_{\text{in}}) f_1(P) f_2(N) f_3(C) w, v) - (H_a(w, C), v), \quad \forall v \in \mathcal{V}, \quad (11)$$

$$(\frac{d}{dt} N, \phi_1) = (L_N(N, P, C, u), \phi_1), \tag{12}$$

$$(\frac{d}{dt} P, \phi_2) = (L_P(N, P, C, u), \phi_2), \tag{13}$$

$$(\frac{d}{dt} C, \phi_3) = (L_C(N, P, C, u), \phi_3), \tag{14}$$

$\forall \phi_i \in L^2(0, T)$, where L_N, L_P, L_C are defined in (9).

3.2   Properties of the solution

Obviously, functions (2), (4), (5), (6) are bounded

$$g(I_{\text{in}}) = |\frac{\mu_0 I_{\text{in}}}{H_L + I_{\text{in}}}| \le \mu_0,$$

$$f_1(P) = |\frac{k_P [P - P_c]_+}{H_P + [P - P_c]_+}| \le k_P, \quad f_2(N) = |\frac{k_N [N - N_c]_+}{H_N + [N - N_c]_+}| \le k_N,$$

$$f_3(C) = |\frac{1}{1 + e^{\lambda(pH(C) - pH_{dopt})}}| < 1,$$

which leads to

$$|g(I_{\text{in}}) f_1(P) f_2(N) f_3(C)| \le \mu_0 k_P k_N \le K, \tag{15}$$

where we denote a generic constant by K. Furthermore, we note that $0 \le H_a(w, C)/w \le K$ and $H_a(w, C)/w \to K(C)$ as $w \to 0$ where $K(C) \ge 0$.

For a function u we define the negative cut $u_- = \min(u, 0)$ and the positive cut $u_+ = \max(u, 0)$. We need the following lemma in order to prove the uniqueness of the solution.

Lemma 3.1. *If f_1, f_2, f_3 are Lipschitz continuous and bounded, then*

$$|f_1(x_1) f_2(y_1) f_3(z_1) - f_1(x_2) f_2(y_2) f_3(z_2)| \le K \left(|x_1 - x_2| + |y_1 - y_2| + |z_1 - z_2| \right).$$

Proof. This lemma is an easy consequence of the boundedness and Lipschitz continuity. First, we see for two functions,

$$|f_1(x_1) f_2(y_1) - f_1(x_2) f_2(y_2)| \le K(|x_1 - x_2| + |y_1 - y_2|).$$

This follows from

$$|f_1(x_1) f_2(y_1) - f_1(x_2) f_2(y_2)| = |f_1(x_1) f_2(y_1) - f_1(x_1) f_2(y_2) + f_1(x_1) f_2(y_2) - f_1(x_2) f_2(y_2)|$$

$$= |f_1(x_1) \left(f_2(y_1) - f_2(y_2) \right) + f_2(y_2) \left(f_1(x_1) - f_1(x_2) \right)|$$

6

and using Lipschitz continuity

$$\leq K\left(|f_1(x_1)||y_1 - y_2| + |f_2(y_2)||x_1 - x_2|\right)$$

and boundedness of f_1, f_2 implies

$$\leq K\left(|y_1 - y_2| + |x_1 - x_2|\right). \tag{16}$$

For the three functions, the proof proceeds on a similar line. By following similar procedure, the result can be extended to any finite number of functions. $\square$

Remark 3.1. *By an abuse of notation, we identify the function g in (2) as $g(\int_0^z w)$. Since g is formed as a composition of two Lipschitz functions, namely Monod and exponential, we conclude that g satisfies,*

$$|g(\int_0^z w_1) - g(\int_0^z w_2)| \leq K|\int_0^z (w_1 - w_2)| \leq K|\int_0^{z_{max}} (w_1 - w_2)|.$$

With this, Lemma 3.1 in particular implies

$$\left(g(\int_0^z w_1)f_1(N_1)f_2(P_1)f_3(C_1) - g(\int_0^z w_2)f_1(N_2)f_2(P_2)f_3(C_2)\right)$$
$$\leq K\left(\int_0^{z_{max}} |w_1 - w_2| + |N_1 - N_2| + |P_1 - P_2| + |C_1 - C_2|\right). \tag{17}$$

$$|L_N(w_1, N_1, P_1, C_1) - L_N(w_2, N_2, P_2, C_2)|$$
$$\leq K\left(|\int_0^{z_{max}} |w_1 - w_2| + |N_1 - N_2| + |P_1 - P_2| + |C_1 - C_2|\right). \tag{18}$$

Similarly for L_P and L_C, we have

$$|L_P(w_1, N_1, P_1, C_1) - L_P(w_2, N_2, P_2, C_2)|$$
$$\leq K\left(|\int_0^{z_{max}} |w_1 - w_2| + |N_1 - N_2| + |P_1 - P_2| + |C_1 - C_2|\right), \tag{19}$$

$$|L_C(w_1, N_1, P_1, C_1) - L_C(w_2, N_2, P_2, C_2)|$$
$$\leq K\left(|\int_0^{z_{max}} |w_1 - w_2| + |N_1 - N_2| + |P_1 - P_2| + |C_1 - C_2|\right). \tag{20}$$

3.3 Existence of a solution

We follow ideas from [15] to use the fixed point operator argument to prove existence. We define a fixed point operator and prove that it is well-defined and continuous. We also prove that this fixed point maps a compact set into itself and using Schauder's fixed point theorem we obtain existence. We define a fixed point operator $\mathcal{T}$:

$$\mathcal{T} : u \mapsto w,$$

with

$$u \in \mathcal{K} := \{u \in L^2(0, T; H^1(\Omega)), \partial_t u \in L^2(0, T; H^{-1}(\Omega)), \quad 0 \le u \le Me^{KT})\}$$

where w together with (N, P, C) solves the following system

$$(\partial_t w, v) + (D_M \partial_z w, \partial_z v) = (g(I_{\text{in}}) f_1(P) f_2(N) f_3(C) w, v) - (\frac{H_a(u, C)}{u} w, v), \quad \forall v \in \mathcal{V},$$

$$(\frac{d}{dt} N, \phi_1) = (L_N(N, P, C, u), \phi_1),$$

$$(\frac{d}{dt} P, \phi_2) = (L_P(N, P, C, u), \phi_2), \tag{21}$$

$$(\frac{d}{dt} C, \phi_3) = (L_C(N, P, C, u), \phi_3),$$

for all $\phi_i \in L^2(0, T)$. In this way we have defined an operator and we first show that

$$\mathcal{T} : \mathcal{K} \mapsto L^2(0, T; H^1(\Omega)) \bigcap H^1(0, T; L^2(\Omega)).$$

Furthermore, note that $\mathcal{K}$ is a compact set with respect to strong L^2 topology. For a given $u \in \mathcal{K}$, first N, P and C are computed and using this from the first equation (21):1, w is computed. Clearly, a fixed point u of this operator together with the corresponding N, P, C solves the system. To obtain this fixed map, we derive a priori estimates, and estimate $\mathcal{T}u_1 - \mathcal{T}u_2$ in terms of $u_1 - u_2$ to prove the continuity of $\mathcal{T}$. To simplify notation, denote

$$F := g(\int_0^z u) f_1(P) f_2(N) f_3(C)$$

and note that $|F| \le K$.

Lemma 3.2. *Operator $\mathcal{T}$ is well-defined and $\mathcal{T}u \in \mathcal{K}$.*

Proof. For $u \in \mathcal{K}$, (21):2, (21):3, (21):4 are ordinary differential equations with Lipschitz right hand side and therefore have unique solution N, P, C. Also for these solutions

$$F - \frac{H_a(u, C)}{u} \le K$$

for $u \in L^2(\Omega)$ and hence the linear parabolic equation (21):1 (linear w.r.t. w) has a unique weak solution and for $u \in \mathcal{K}$, $\mathcal{T}u \in L^2(0, T; H^1(\Omega)) \bigcap H^1(0, T; L^2(\Omega))$.

To see that $0 \leq \mathcal{T}u \leq Me^{KT}$, we first choose $v = w_-$ and obtain

$$(\partial_t w, w_-) + (D_M \partial_z w, \partial_z w_-) = (Fw, w_-) - (\frac{H_a(u, C)}{u} w, w_-)$$

and hence,

$$\frac{d}{dt}||w_-||^2 \leq K||w_-||^2$$

leading to $w \geq 0$. Similarly, test with $[w - Me^{KT}]_+$ to obtain $\mathcal{T}u \in \mathcal{K}$. $\qquad \square$

Lemma 3.3. $\mathcal{T}$ *is a continuous operator.*

Proof. To estimate $\mathcal{T}u_1 - \mathcal{T}u_2$ we use the system of equations. For $u = u_1 - u_2$ we obtain for all $v \in \mathcal{V}$

$$(\partial_t(w_1 - w_2), v) + (D_M \partial_z(w_1 - w_2), \partial_z v)$$
$$= (F_1 w_1 - F_2 w_2, v) - (\frac{H_a(u_1, C_1)}{u_1} w_1 - \frac{H_a(u_2, C_2)}{u_2} w_2, v),$$

where $F_i = g(\int_0^z u_i) f_1(P_i) f_2(N_i) f_3(C_i)$. Consider the first equation,

$$(\partial_t(w_1 - w_2), v) + (D_M \partial_z(w_1 - w_2), \partial_z v) = (F_1 w_1 - F_2 w_2, v) - (\frac{H_a(u_1, C_1)}{u_1} w_1 - \frac{H_a(u_2, C_2)}{u_2} w_2, v),$$

and use $v = w_1 - w_2$ as the test function to obtain

$$(\partial_t(w_1 - w_2), w_1 - w_2) + (D_M \partial_z(w_1 - w_2), \partial_z(w_1 - w_2))$$
$$= (F_1 w_1 - F_2 w_2, w_1 - w_2) - (\frac{H_a(u_1, C_1)}{u_1} w_1 - \frac{H_a(u_2, C_2)}{u_2} w_2, w_1 - w_2).$$

The first term of the right hand side can be estimated as follows,

$$(F_1 w_1 - F_2 w_2, w_1 - w_2)$$

$$= (g(\int_0^z u_1) f_1(N_1) f_2(P_1) f_3(C_1) w_1 - g(\int_0^z u_2) f_1(N_2) f_2(P_2) f_3(C_2) w_2, w_1 - w_2)$$

$$= (g(\int_0^z u_1) f_1(N_1) f_2(P_1) f_3(C_1)(w_1 - w_2), w_1 - w_2)$$

$$+ (w_2(g(\int_0^z u_1) f_1(N_1) f_2(P_1) f_3(C_1) - g(\int_0^z u_2) f_1(N_2) f_2(P_2) f_3(C_2)), w_1 - w_2)$$

9

$$\leq K||w_1 - w_2||^2 + (w_2(g(\int_0^z u_1)f_1(N_1)f_2(P_1)f_3(C_1) - g(\int_0^z u_2)f_1(N_2)f_2(P_2)f_3(C_2)), w_1 - w_2)$$

$$\leq K||w_1 - w_2||^2 + K||w_1 - w_2||(||u_1 - u_2|| + ||N_1 - N_2|| + ||P_1 - P_2|| + ||C_1 - C_2||)$$

$$\leq K \left(||w_1 - w_2||^2 + ||u_1 - u_2||^2 + ||N_1 - N_2||^2 + ||P_1 - P_2||^2 + ||C_1 - C_2||^2 \right).$$

For the second term, note that $\frac{H_a(u,C)}{u}$ is uniformly bounded and Lipschitz in C and hence can be bounded by

$$(\frac{H_a(u_1, C_1)}{u_1} w_1 - \frac{H_a(u_2, C_2)}{u_2} w_2, w_1 - w_2) \leq K(||w_1 - w_2||^2 + ||C_1 - C_2||^2)$$

and hence, we have

$$\frac{d}{dt}||w_1 - w_2||^2 \leq K \left(||w_1 - w_2||^2 + ||u_1 - u_2||^2 + ||N_1 - N_2||^2 + ||P_1 - P_2||^2 + ||C_1 - C_2||^2 \right)$$

and for $||u_1 - u_2|| \to 0$, we conclude using Gronwall's lemma and continuity of solutions of ODEs for $(N_1, P_1, C_1), (N_2, P_2, C_2)$ that $||w_1 - w_2|| \to 0$. $\qquad\square$

Lemma 3.4. *There exists a solution (w, N, P, C) of the weak formulation* (11)-(14).

Proof. Since $\mathcal{T}$ maps a compact set $\mathcal{K}$ to itself and is continuous, using Schauder's fixed point theorem there exists a fixed point $w \in \mathcal{K}$ such that

$$\mathcal{T}w = w$$

which implies the existence of the solution for the weak formulation (11)-(14). $\qquad\square$

3.4 Positivity

Lemma 3.5 (Positivity of w, N, P, C). *If the initial conditions $w(z, 0), N(0), P(0), C(0) \geq 0$, then the solution of* (11)-(14) *$w(z, t), N(t), P(t), C(t) \geq 0$.*

Proof. The case for w is trivial as $w \in \mathcal{K}$. Next, we consider the case for N and note that $0 \leq L_N(w, N, P, C) \leq KN$. In the weak formulation,

$$(\frac{d}{dt}N, \phi_1) = (L_N(w, N, P, C), \phi_1),$$

choose $\phi_1 = N_-$ (where N_- is the negative cut of N) to obtain

$$\frac{d}{dt}||N_-||^2 \leq K||N_-||^2$$

and using the initial condition $||N_-||_{t=0} = 0$ and Gronwall's lemma, we conclude,

$$N(t) \geq 0.$$

The proofs for P and C follow similar arguments. $\qquad\square$

3.5 Boundedness

Lemma 3.6. *If the initial condition is bounded* $w(z,0), N(0), P(0), C(0) \leq M$, *then the solution of* (11)-(14) *remains bounded that is,* $w(z,t), N(t), P(t), C(t) \leq Me^{Kt}$.

Proof. Once again the case for w is straightforward as it inherits this property from the set $\mathcal{K}$. Next we consider the case for N, P, C. Use $\phi_1 = [N - Me^{Kt}]_+$ in the weak formulation to obtain,

$$(\frac{d}{dt}N, [N - Me^{Kt}]_+) = (L_N(w, N, P, C), [N - Me^{Kt}]_+)$$

and rewrite the left hand side,

$$(\frac{d}{dt}N, [N - Me^{Kt}]_+) = (\frac{d}{dt}(N - Me^{Kt}), [N - Me^{Kt}]_+) + (MKe^{Kt}, [N - Me^{Kt}]_+)$$

and hence,

$$\frac{d}{dt}||[N - Me^{Kt}]_+||^2 = (L_N(w, N, P, C), [N - Me^{Kt}]_+) - (MKe^{Kt}, [N - Me^{Kt}]_+)$$

which leads to

$$\frac{d}{dt}||[N - Me^{Kt}]_+||^2 \leq 2K(N - MKe^{Kt}, [N - Me^{Kt}]_+) \leq 2K||[N - Me^{Kt}]_+||^2$$

and together with initial condition, $||[N - Me^{Kt}]_+|| = 0$ and Gronwall's lemma proves the assertion. The proofs for P and C are similar. $\qquad\square$

3.6 Uniqueness

Lemma 3.7 (Uniqueness of weak solution). *Assume* $(w_1, N_1, P_1, C_1), (w_2, N_2, P_2, C_2)$ *are two weak solutions of* (1)-(10) *corresponding to the same initial data, then* $(w_1, N_1, P_1, C_1) \equiv (w_2, N_2, P_2, C_2)$.

Proof. If possible, let $\{w_1, N_1, P_1, C_1\}$ and $\{w_2, N_2, P_2, C_2\}$ be two weak solutions for the same initial data. Hence, both these satisfy the weak form

$$(\partial_t w_1, v) + (D_M \partial_z w_1, \partial_z v) = (g(I_{\text{in}})f_1(P_1)f_2(N_1)f_3(C_1)w_1, v) - (H_a(w_1), v), \quad \forall v \in \mathcal{V},$$

$$(\frac{d}{dt}N_1, \phi_1) = (L_N(N_1, P_1, C_1, w_1), \phi_1),$$

$$(\frac{d}{dt}P_1, \phi_2) = (L_P(N_1, P_1, C_1, w_1), \phi_2),$$

$$(\frac{d}{dt}C_1, \phi_3) = (L_C(N_1, P_1, C_1, w_1), \phi_3),$$

(22)

$\forall \phi_i \in L^2(0, T)$.

$$(\partial_t w_2, v) + (D_M \partial_z w_2, \partial_z v) = (g(I_{\text{in}}) f_1(P_2) f_2(N_2) f_3(C_2) w_2, v) - (H_a(w_2), v), \quad \forall v \in \mathcal{V},$$

$$(\frac{d}{dt} N_2, \phi_1) = (L_N(N_2, P_2, C_2, w_2), \phi_1),$$

$$(\frac{d}{dt} P_2, \phi_2) = (L_P(N_2, P_2, C_2, w_2), \phi_2), \tag{23}$$

$$(\frac{d}{dt} C_2, \phi_3) = (L_C(N_2, P_2, C_2, w_2), \phi_3),$$

$\forall \phi_i \in L^2(0, T)$. Note that $w_1 - w_2, \; N_1 - N_2, P_1 - P_2, C_1 - C_2$ have zero initial data.

Subtract (23) from (22) and choose for the test functions $v = w_1 - w_2, \phi_1 = N_1 - N_2, \phi_2 = P_1 - P_2, \phi_3 = C_1 - C_2$ to obtain

$$\frac{d}{dt} \left(||w_1 - w_2||^2 + ||N_1 - N_2||^2 + ||P_1 - P_2||^2 + ||C_1 - C_2||^2 \right)$$

$$= (g(\int_0^z w_1) f_1(N_1) f_2(P_1) f_3(C_1) w_1 - g(\int_0^z w_2) f_1(N_2) f_2(P_2) f_3(C_2) w_2, w_1 - w_2)$$

$$+ (L_N(w_1, N_1, P_1, C_1) N_1 - L_N(w_2, N_2, P_2, C_2) N_2, N_1 - N_2)$$

$$+ (L_P(w_1, N_1, P_1, C_1) N_1 - L_P(w_2, N_2, P_2, C_2) N_2, P_1 - P_2)$$

$$+ (L_C(w_1, N_1, P_1, C_1) N_1 - L_C(w_2, N_2, P_2, C_2) N_2, C_1 - C_2).$$

Denote the first term of the right hand side by $I_i, \quad i = 1, 2, 3, 4$. We treat I_1 first,

$$(g(\int_0^z w_1) f_1(N_1) f_2(P_1) f_3(C_1) w_1 - g(\int_0^z w_2) f_1(N_2) f_2(P_2) f_3(C_2) w_2, w_1 - w_2)$$

$$= (g(\int_0^z w_1) f_1(N_1) f_2(P_1) f_3(C_1)(w_1 - w_2), w_1 - w_2)$$

$$+ (w_2(g(\int_0^z w_1) f_1(N_1) f_2(P_1) f_3(C_1) - g(\int_0^z w_2) f_1(N_2) f_2(P_2) f_3(C_2)), w_1 - w_2)$$

$$\leq K||w_1 - w_2||^2 + (w_2(g(\int_0^z w_1) f_1(N_1) f_2(P_1) f_3(C_1) - g(\int_0^z w_2) f_1(N_2) f_2(P_2) f_3(C_2)), w_1 - w_2)$$

$$\leq K||w_1 - w_2||^2 + K||w_1 - w_2||(||N_1 - N_2|| + ||P_1 - P_2|| + ||C_1 - C_2||).$$

For the last inequality, we have used (17) and Cauchy-Schwarz and the pointwise boundedness of w_2. The constant K depends on final time T. Furthermore, we use Young's inequality to obtain

$$|I_1| \leq K(T) \left(||w_1 - w_2||^2 + ||N_1 - N_2||^2 + ||P_1 - P_2||^2 + ||C_1 - C_2||^2 \right).$$

For I_2, we use (18), Cauchy-Schwarz and Young's inequality to get

$$|I_2| \leq K(T) \left(||w_1 - w_2||^2 + ||N_1 - N_2||^2 + ||P_1 - P_2||^2 + ||C_1 - C_2||^2 \right).$$

And similarly, for I_3, I_4.

Hence,

$$\frac{d}{dt} \left(||w_1 - w_2||^2 + ||N_1 - N_2||^2 + ||P_1 - P_2||^2 + ||C_1 - C_2||^2 \right)$$

$$\leq K(T) \left(||w_1 - w_2||^2 + ||N_1 - N_2||^2 + ||P_1 - P_2||^2 + ||C_1 - C_2||^2 \right)$$

and using Gronwall's lemma and zero initial condition for $w_1 - w_2, N_1 - N_2, P_1 - P_2, C_1 - C_2$ leads to

$$||w_1 - w_2||^2 + ||N_1 - N_2||^2 + ||P_1 - P_2||^2 + ||C_1 - C_2||^2 = 0$$

and thus, the assertion for the uniqueness of weak solution for the system. $\square$

4 Numerical solution of the model

In this section we discuss the numerical solution approach for the algae growth model. We use the method of lines (MOL) approach which consists of two stages. The first stage is the spatial discretization in which the spatial derivatives of the PDE are discretized, for example with finite differences, finite volumes or finite element schemes. By discretizing the spatial operators, the PDE with its boundary conditions is converted into a system of ODEs in $\mathbb{R}^m$

$$\boldsymbol{W}'(t) = \boldsymbol{F}\left(t, \boldsymbol{W}(t)\right), \quad \boldsymbol{W}(0) = \boldsymbol{W}_0, \tag{24}$$

called the semi-discrete system. This ODE system is still continuous in time and needs to be integrated. So, the second stage in the numerical solution is the numerical time integration of system (24). At this stage the approximations $\boldsymbol{W}_n$ at time levels t_n are computed. The discretization of the diffusion term in (1) results in a contribution proportional to $D_M/\Delta x^2$, where Δx denotes the spatial grid size. Thus, for fine grids system (24) becomes stiff and implicit time integration methods have to be considered.

Since our model describes the relation between the algae concentration and concentrations of phosphates, nitrates and CO_2 which are all positive quantities, it is important that the time integration method possesses the positivity preservation property. With positivity preservation we mean that the numerical solution vector $\boldsymbol{W}_n \geq 0$, $\forall t > 0$ if the initial solution $\boldsymbol{W}_0 \geq 0$.

In this section we will assume that there exist a $\tau_0 > 0$ such that

$$\boldsymbol{v} + \tau \boldsymbol{F}(t, \boldsymbol{v}) \geq 0 \quad \text{for all} \quad \boldsymbol{v} \geq 0, \quad t \geq 0, \quad 0 < \tau < \tau_0. \tag{25}$$

We will look for a two-step method

$$\boldsymbol{W}_n = \sum_{k=1}^{2} a_k \boldsymbol{W}_{n-k} + \tau \sum_{k=0}^{2} b_k \boldsymbol{F}\left(t_{n-k}, \boldsymbol{W}_{n-k}\right) \tag{26}$$

13

which preserves positivity. For consistency, the condition

$$a_1 + a_2 = 1 \tag{27}$$

has to be satisfied. If $b_0 \neq 0$ then the method is implicit. Second-order methods of type (26) form a two-parameter family with coefficients

$$a_1 = 2 - \xi, \quad a_2 = \xi - 1, \quad b_0 = \eta, \quad b_1 = 1 + \frac{1}{2}\xi - 2\eta, \quad b_2 = \eta + \frac{1}{2}\xi - 1. \tag{28}$$

The method is zero-stable if $\xi \in (0, 2]$ and is A-stable if we also have $\eta \geq \frac{1}{2}$.

We introduce the following sublinear functional

$$||\boldsymbol{v}||_0 = -\min(v_1, \ldots, v_m, 0). \tag{29}$$

It is easily seen that $||\boldsymbol{v}||_0$ is nonnegative.

We also observe that the positivity of the starting vectors $\boldsymbol{v}_0$ and $\boldsymbol{v}_1$ together with the existence of a bound $\mu > 0$, such that the boundedness property

$$||\boldsymbol{v}_n||_0 \leq \mu \cdot \max_{0 \leq j \leq 1} ||\boldsymbol{v}_j||_0, \qquad \text{for all } n \geq 2 \tag{30}$$

holds, guarantees the positivity of the numerical solution.

Using the results from [8] we can write the conditions which would imply the boundedness property (30). We denote by m the number of steps performed with the method (26), by E the backward shift matrix

$$E = \begin{pmatrix} 0 & & & \\ 1 & 0 & & \\ & \ddots & \ddots & \\ & & 1 & 0 \end{pmatrix} \in \mathbb{R}^{m \times m}, \tag{31}$$

and

$$A = \sum_{j=1}^{2} a_j E^j, \quad B = \sum_{j=0}^{2} b_j E^j. \tag{32}$$

From [8] it follows that if for a $\gamma > 0$ and a zero-stable method (26) we have

$$P = (I - A + \gamma B)^{-1} \gamma B > 0 \quad \text{for all } m \tag{33}$$

then there exist a $\mu > 0$ such that boundedness property (30) is satisfied for any $\tau \leq \gamma \tau_0$. In (33) the inequality should be satisfied element wise. We mention that this result was derived for the case when the function $\boldsymbol{F}$, the sublinear functional (29) and the initial solution $\boldsymbol{W}_0$ are unknown. In practice we can still have positivity preservation by allowing the use of larger time steps.

In order to ease the verification of the condition (33) we decompose P as

$$P = (I - A + \gamma B)^{-1} \gamma B = \sum_{j \geq 0} \pi_j E^j, \tag{34}$$

where

$$\pi_n = \gamma \sum_{j=0}^{2} b_j \rho_{n-j} \qquad (n \geq 0) \tag{35}$$

and the coefficients ρ_n satisfy the multiple recursion

$$\rho_n = \sum_{j=1}^{2} a_j \rho_{n-j} - \gamma \sum_{j=0}^{2} b_j \rho_{n-j} + \delta_{n0} \qquad (n \geq 0), \tag{36}$$

with Kronecker delta symbol δ_{n0} and $\rho_j = 0$ for $j < 0$.

For instance, if we consider the BDF2 method [4], obtained for $\xi = \eta = \frac{2}{3}$, the condition (33) is satisfied for all γ for which all the elements of the sequence defined by the recurrence relation

$$\rho_{n+2} = \frac{1}{3 + 2\gamma} (4\rho_{n+1} - \rho_n) \tag{37}$$

with

$$\rho_0 = \frac{3}{3 + 2\gamma}, \qquad \rho_1 = \frac{12}{(3 + 2\gamma)^2} \tag{38}$$

are strictly positive.

For $\gamma = \frac{1}{2}$ the sequence (37) is defined by

$$\rho_n = \frac{3(n+1)}{2^{n+2}} > 0 \quad \text{for all } n, \tag{39}$$

whereas for $\gamma > \frac{1}{2}$ it is easy to show that the strict positivity of the elements ρ_n does not hold anymore. Thus, for the BDF2 method the largest value of γ which satisfies (33) is $\gamma = \frac{1}{2}$.

5 Numerical experiment

In this section we test our model for the set of parameters presented in the Section 1.

We discretize the diffusion operator in (1) by standard second-order central differences on a fixed uniform grid $0 = z_1 < z_2 < \ldots < z_m = z_{max}$. The integral term within the light function (3) is approximated by

$$\int_0^{z_k} w \, dz_k \approx \frac{z_k}{k} \sum_{i=1}^{k} z_i.$$

The other integral term used in (9) is approximated by

$$\int_0^{z_{\max}} g(I_{\text{in}})f_1(P)f_2(N)f_3(C)wdz \approx \frac{z_{\max}}{m}f_1(P)f_2(N)f_3(C)\sum_{i=1}^{m}g(I_{\text{in}}(z_i,t))z_i \,.$$

The obtained system (24) is stiff due to the diffusion term, therefore, an implicit numerical integration method must be used. We use the two-step implicit BDF2 method [4].

An illustration of the algae concentration in time is given in Figure 3. The behavior in time of P, N, C and pH is presented in Figure 4 and Figure 5.
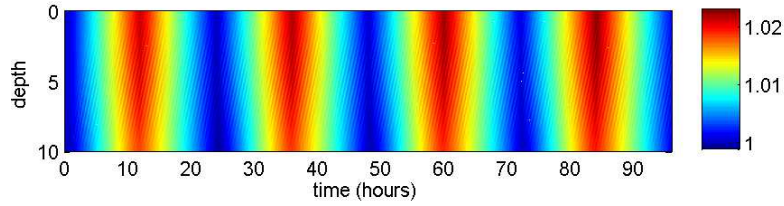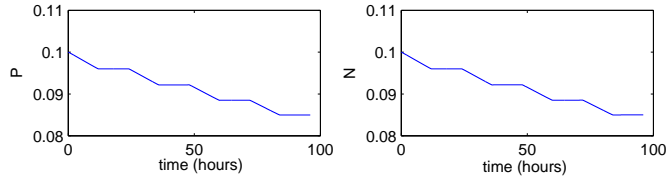

Figure 3: Concentration of algae.
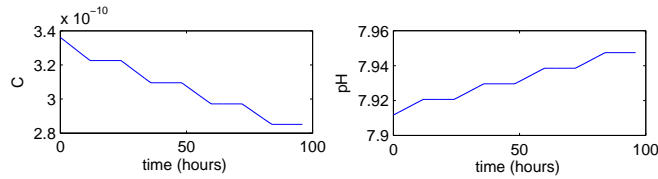

Figure 4: Concentration of P and N.

Figure 5: Concentration of C and pH.

The model equations (1),(9)-(10) are discretized and solved in the domain $z \in [0, z_{max}]$ on the interval $t \in [0, T]$, where $T = 96$ $[hours]$, which corresponds to 4 days. Minerals are being added with a constant rate of $3.64 \cdot 10^{-10}$ $[mol/(l \cdot s)]$ and $2.78 \cdot 10^{-10}$ $[mol/(l \cdot s)]$ for N and P respectively. No carbon dioxide is added. In Figure 3 we notice the periodic nature of the algae concentration. This is due to the day-night cycle of the external illumination

modeled by $I_0(t)$. The decay of light intensity with depth makes the solution z-dependent. As expected, the algae concentration is lower at the bottom. However, the mixing included in the model diminishes this difference. Due to a large initial concentration of algae, the rate of consumption of minerals is larger than their inflow rate. There is no inflow of carbon dioxide. Thus, the concentration of minerals and of carbon dioxide in the water decreases monotonically as seen from Figure 4 and Figure 5. During one day, the maximum algae concentration is attained in the noon when the light intensity on the surface is the largest. In this particular simulation the value of the maximal concentration increases from day to day at a rate which is comparable with literature data.

6   Optimization

We define the average concentration of algae

$$V = \frac{1}{z_{max}T} \int_0^{z_{max}} \int_0^T w(z,t)dtdz,$$

or in discrete form

$$V \approx \frac{1}{nm} \sum_{j=1}^n \sum_{i=1}^m w(z_i, t_j),$$

where t_i are the time points in which the numerical solution is computed. The average concentration computed by means of the model described above can be optimized as a function of three design variables: carbon dioxide, nitrate and phosphate inflow rates, i.e.

$$\text{maximize } V(S_C, S_N, S_P),$$

$$\text{subject to } S_C \geq 0, S_N \geq 0, S_P \geq 0.$$

For this purpose we apply the Nelder-Mead simplex method [1, 13]. The Nelder-Mead simplex method is designed to find a local optimum of a function. It makes no assumptions about the shape of the function and does not use derivative information. At each iteration the Nelder-Mead simplex method evaluates the function in a finite number of points. In our case one function evaluation corresponds to computing the average concentration of algae.

Figure 6 shows an example of the Nelder-Mead optimization. In this case the optimization required 55 function evaluations. The values of the design variables and correspondingly obtained concentration are plotted for each function evaluation. Table 1 shows the values of the initial guess and the values after optimization. For the optimized values of the design variables the average algae concentration has increased by 7.03%.

Further, the result of the optimization could be improved by assuming S_C, S_N, S_P to be functions of time. Thus, we assume that $\mathbf{s}_C = \{S_{C,i}\}_{i=1}^L$, where $S_{C,i}$ is the carbon dioxide inflow rate at time t_i. For fixed S_N and S_P we obtain an optimization problem of L design variables
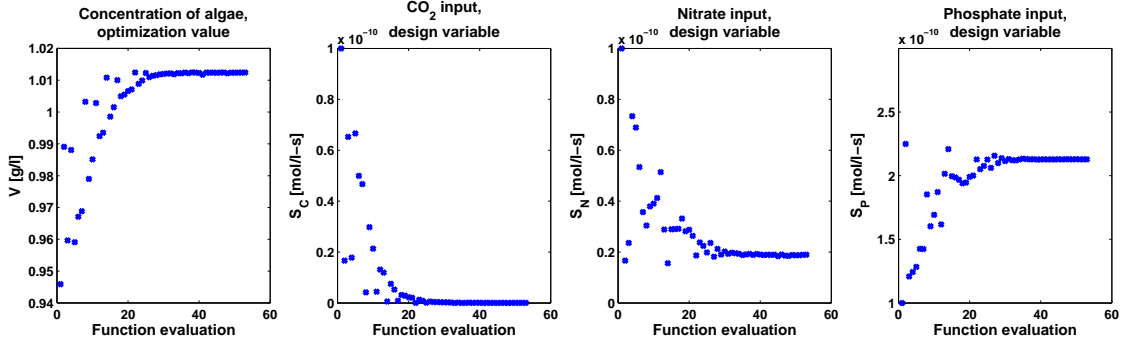
$$\text{maximize } V(\mathbf{s}_C),$$

Figure 6: Nelder-Mead simplex optimization.

Table 1: Optimization parameters.

	S_C [mol/(l-s)]	S_N [mol/(l-s)]	S_P [mol/(l-s)]	V [g/l]
Initial	10^{-10}	10^{-10}	10^{-10}	0.946
Optimized	5.309×10^{-14}	1.886×10^{-11}	2.129×10^{-10}	1.0125

$$\text{subject to } S_{C,i} \geq 0.$$

This could result in further improvement of the average algae concentration. As an initial guess for optimization, instead of applying constant carbon dioxide inflow rate, we could use a periodic function with the same period as of the incident light function, with different amplitude and vertical and horizontal shift (see Figure 7).

It is important to note that the average algae concentration function may have multiple maxima. However, the Nelder-Mead simplex method is designed to find a local optimum of a function. It means that initial parameter guess should be close enough to the desirable optimum. For a global optimum other optimization methods (for example, simulated annealing optimization [13]) could be used.
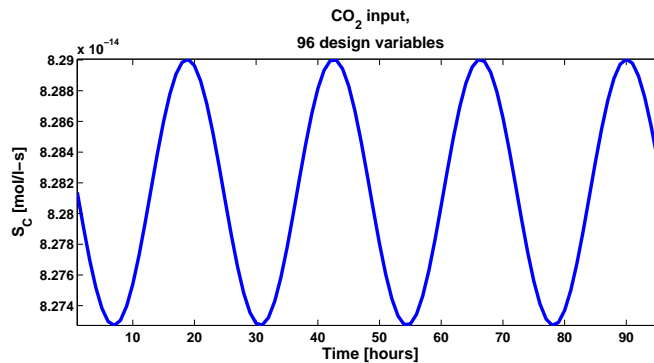

Figure 7: Input of CO_2 as a function of time.

18

7 Conclusions

We proposed a model for the growth of algae in a mineral solution. The model consists of a partial differential equation for the algae concentration coupled to three ordinary differential equations for the phosphate, the nitrate and the carbon dioxide concentrations. The minerals and the carbon dioxide are assumed to have a constant concentration throughout the volume, while the algae concentration is modeled as a z-dependent quantity. This choice is explained by the strong dependence of light intensity on depth. Moreover, the z-dependency allows us to study the effect of mixing on the algae population. Numerical simulations were performed with the model. To this end, the continuous equations are discretized in space by a finite difference scheme, and the resulting system of ordinary differential equations is integrated in time by a two-step implicit BDF2 method. The simulations have shown a good qualitative prediction for the concentration of algae, minerals and carbon dioxide. In order to achieve also a good quantitative prediction, the parameters of the model have to be adjusted to the experiment. Based on the proposed model, the average concentration of the algae can be optimized by means of derivative-free optimization.

Acknowledgement

References

[1] A.R. Conn, K. Scheinberg, L.N. Vicente, *Introduction to derivative-free optimization.* MPS-SIAM series on optimization, Philadelphia, 2009.

[2] C.S. Duke, W. Litaker, J. Ramus, *Effect of temperature on nitrogen-limited growth rate and chemical composition of Ulva curvata.* Marine Biology 100,143–150, 1989.

[3] H. Haario, L. Kalachev, M. Laine, *Reduced Models of Algae Growth.* Bulletin of Mathematical Biology 71, 1626–1648, 2009.

[4] E. Hairer, G. Wanner, *Solving Ordinary Differential Equations II – Stiff and Differential-Algebraic Problems.* Second edition, Springer Series in Comp. Math. 14, Springer, 1996.

[5] J. Huisman, R.R. Jonker, C. Zonneveld, F.J. Weissing, *Competition for light between phytoplankton species, experimental tests of mechanistic theory.* Ecology 80, 211–222, 1999.

[6] J. Huisman, N.N. Pham Thi, D.M. Karl, B. Sommeijer, *Reduced mixing generates oscillations and chaos in the oceanic deep chlorophyll maximum.* Nature 439, 322–325, 2006.

[7] J. Huisman, F.G. Weissing, *Light-Limited Growth and Competition for Light in Well-Mixed Aquatic Environments: An Elementary Model.* Ecology 75 (2), 507–520, 1994.

[8] W. Hundsdorfer, A. Mozartova, M.N. Spijker, *Stepsize restrictions for boundedness and monotonicity of multistep methods*, CWI report, MAC-1004, 2010.

[9] W. Hundsdorfer, J.G. Verwer, *Numerical Solution of Time-Dependent Advection-Diffusion-Reaction Equations.* Springer Series in Comp. Math. 33, Springer, 2003.

[10] O. Malve, M. Laine, H. Haario, T. Kirkkala, J. Sarvala, *Bayesian modelling of algal mass occurrences-using adaptive MCMC methods with a lake water quality model.* Ecology 22 (7), 966–977, 2007.

[11] N.N. Pham Thi, *Numerical Analysis of Phytoplankton Dynamics.* PhD thesis, University of Amsterdam, 2006.

[12] N. N. Pham Thi, J. Huisman, B. P. Sommeijer, *Simulation of three-dimensional phytoplankton dynamics: competition in light-limited environments.* Journal of Computational and Applied Mathematics 174 (1), 57–77, 2005.

[13] W.H. Press, S.A. Teukolsky, W.T. Vetterling, *Numerical Recipes: the Art of Scientific Computing.* third ed., Cambridge University Press, Cambridge, 2007.

[14] I.S. Pop, T.L. van Noorden, A. Ebigbo , R. Helmig, *An effective model for biofilm growth in a thin strip.* Water Resour. Res., Vol. 46 (2010), W06505, doi:10.1029/2009WR008217.

[15] I.S. Pop, C J van Duijn, *Crystal dissolution and precipitation in porous media: pore scale analysis.* J. Reine Angew. Math. Vol. 577 (2004), pp. 171–211.

PREVIOUS PUBLICATIONS IN THIS SERIES:

Number	Author(s)	Title	Month
10-70	T. Fatima A. Muntean	Sulfate attack in sewer pipes: Derivation of a concrete corrosion model via two-scale convergence	Nov. '10
10-71	M.E. Rudnaya R.M.M. Mattheij J.M.L. Maubach	Orientation identification of the power spectrum	Dec. '10
10-72	V. Savcenco B. Haut	A multirate approach for time domain simulation of very large power systems	Dec. '10
10-73	O. Matveichuk J.J.M. Slot	A Rouse-like model for highly ordered main-chain liquid crystalline polymers containing hairpins	Dec. '10
10-74	K. Kumar M. Pisarenco M. Rudnaya V. Savcenco	Analysis, numerics, and optimization of algae growth	Dec. '10